J|A|C|S COMMUNICATIONS

Published on Web 06/04/2010

Differing HOMO and LUMO Mediated Conduction in a Porphyrin Nanorod

Benjamin A. Friesen, Bryan Wiggins, Jeanne L. McHale, Ursula Mazur,* and K. W. Hipps*

Washington State University, Department of Chemistry and Materials Science and Engineering Program, P.O. Box 644630, Pullman, Washington 99164-4630

Received April 12, 2010; E-mail: hipps@wsu.edu

There has been considerable recent interest in the production of porphyrin self-assembled nanostructures.[1,2] Although porphyrin materials in general are known to be photoconductors[3] as well as photovoltaics[4] and capable of light-induced charging,[5] there has been very little reported in terms of the conducting properties of their self-assembled nanostructures. To our knowledge, Schwab and co-workers[6] have provided the only electronic transport study of self-assembled porphyrin nanostructures to date. They reported on the photoconductivity of nanorods formed from highly acidic solutions of meso-tetrakis(4-sulfonato-phenyl)porphine. Schwab et al.[6] found that the photoconductivity grows over hundreds of seconds upon light exposure and decays slowly when the light is off. They proposed a qualitative model where the conduction occurred through the LUMOs of the molecules. They also reported that the rods were insulating over the voltage range studied (±0.5 V) in the dark.

In addition to the dearth of electronics studies of porphyrin nanostructures, there is also a conspicuous shortage of scanning tunneling microscopy, STM, work. Friesen et al. reported the only detailed STM images available to date [also on meso-tetrakis(4-sulfonatophenyl)porphine].[2] Their work was performed in air. By contrasting STM and AFM images, they inferred that the nanorods were highly conducting at voltages above approximately +1.5 V relative to the substrate. In this communication we will provide the first UHV-STM images, STM-based current−voltage ($I-V$) curves, and orbital mediated tunneling spectroscopy[7] (OMTS) of a self-assembled porphyrin nanostructure at the level of a single nanorod or single molecule constituent. We will show that transverse conductivity over distances less than 10 nm can occur by barrier type tunneling but that long distance conduction solely occurs through the LUMO band.

The HCl adduct of the meso-tetrakis(4-sulfonato-phenyl)porphine HCl, $H_2(H_4TSPP)\cdot 2HCl$, was purchased from Porphyrin Products and used as supplied. Either a 1×10^{-6} M or 5×10^{-6} M solution was freshly prepared in 0.75 M HCl. These solutions were then placed on either HOPG or Au(111) surfaces and allowed to stand for 45 or 60 min, respectively. Then the substrates were spun dry. AFM and STM images in air showed rods that were approximately 4 nm high, 27 nm wide, and 0.3 to 2 μm long. These sizes are consistent with those reported previously whether made using the sodium salt as starting material[2] or using the HCl adduct.[6] All samples were transferred to UHV, and some were heated to 100 °C for 9 min before measurement. They were then analyzed either by STM or XPS. $I-V$ and dI/dV spectra were collected in constant height mode. The tip was set at a desired position at a set point of +1.6 V and 15 pA, the feedback was turned off, and 64 $I-V$ curves were collected at the selected point. dI/dV curves were numerically calculated from the $I-V$ curves. $I-V$ and dI/dV curves are averages of those 64 scans. Images were acquired in constant current mode at +1.6 V sample bias and 1 pA set point current. All data were acquired using an RHK variable substrate temperature UHV STM and RHK XPM Pro software.

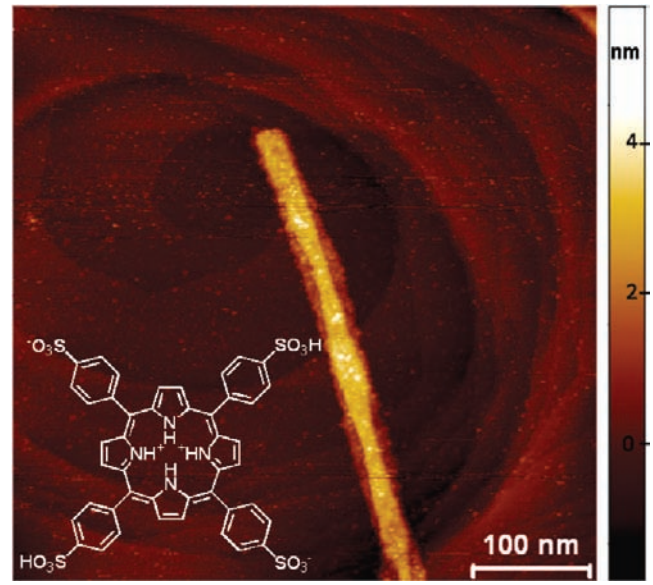

Figure 1. Constant current UHV-STM image of a nanorod on Au(111) taken at a set point of 1.0 pA and 1.5 V sample bias.

XPS samples were prepared with the same procedures as those for the STM samples, but they were not heated in UHV. 180−200 W of achromatic radiation at an energy of 1253.6 eV (Mg Kα) was used as XPS excitation sources. The analyzer was set for a spatial resolution of 120 μm. The energy resolution was set to 1.0 eV for survey spectra and to 0.15 eV for the higher resolution acquisitions of C1s, N1s, S2p, Cl2p, and Au4$f_{7/2}$ peaks. Binding energies were calibrated against the Au4$f_{7/2}$ peak taken to be located at BE = 84.3 eV and against the C1s peaks for HOPG samples (BE = 284.5 eV). For unheated Au(111) samples XPS revealed that chlorine was present on the surface, for both $H_2(H_4TSPP)$ in HCl and HCl alone. They also showed that no chlorine was present on the surface for heated Au(111) samples and no chlorine was detected at any time on HOPG.

Our XPS studies indicated that all four nitrogen atoms were protonated. These results are consistent with previous assumptions that the neutral form of the acid, $H_2(H_4TSPP)$, is the only chemical species in the nanorods. The inset in Figure 1 is the structure of that species. It is thought that the driving force for rod formation is electrostatic interaction between the negative sulfonate and the positive core of adjacent molecules. Sulfonates stack above and below the +2 core of a third molecule to create an extended structure.[1,2]

While there are several proposed structures for the rods that are consistent with this ionic self-assembly pattern,[2,8,9] there is no general agreement on exactly how the molecules form the observed

10.1021/ja103078q

rods. It should be noted that there is good evidence that these "rods" are actually collapsed nanotubes. For example, Vlaming and co-workers have recently shown Cryo-EM images of these nanostructures in frozen solution that are clearly tubes of 18 nm diameter and ~2 nm thick.[8] In some of our STM images, we have also seen evidence that the 4 nm thick rods are actually collapsed tubes having 2 nm thick walls.

A typical large UHV-STM image of a portion of a nanorod on Au(111) is presented in Figure 1. The STM images of areas off the rod are consistently rough (on a 0.1 nm scale) and noisy. Moreover, the characteristic reconstruction on Au(111) was seen before deposition but was not observable after deposition. Au(111) substrates treated with 0.75 M HCl (only) for the same 1 h period have a similar appearance. Images taken with HOPG as substrate did not have this problem. Since the XPS results clearly show a surface reaction between HCl and Au(111), and because HOPG is free from chloride adsorption, we attribute the apparent roughness and poor stability of off-rod STM data as due to the reaction of HCl with Au over the course of the 1 h treatment. It is important to note, however, that the height, width, and length of the nanorods formed on HOPG and on Au(111) were essentially the same. Moreover, $I-V$ curves obtained from rods supported on either substrate were the same. One difference between nanorods on Au(111) and on graphite is the presence on gold of disklike aggregates of the order of 6 nm in diameter.[2] Upon heating to 100 °C in UHV the number and prominence of these structures significantly decreased. While small aggregates were observed on samples prepared on HOPG, they were generally less frequent and more random in size. We are presently working to understand these differences. However, we believe that any results reported here for the UHV properties of the nanorods on HOPG are directly transferable to nanorods supported on Au(111).

Thus, in this communication, we will focus on $I-V$ and OMTS data acquired from HOPG supported samples that have been heated to 100 °C. Figure 2 presents a set of data taken from a region where several rods overlap and it is possible to interrogate 4, 6, 8, and 12 nm thick regions. As indicated earlier, the "rods" appear to be collapsed nanotubes having a wall thickness of 2 nm; thus the 6 nm region would be a full tube overlaid with a half tube. Also shown are $I-V$ curves taken from these varying thickness regions. It is immediately apparent that there is a significant band gap and that the conductivity in negative sample bias decreases dramatically with increasing rod thickness. The lowest graph in Figure 2 shows that the current at −2 V (normalized to the set-point current) decreases exponentially and obeys the relationship $I \propto \exp(-\beta t)$, where t is the thickness in angstroms and $\beta = -0.11/\text{Å}$. This type of dependence is normally associated with single or multiple barrier tunneling or superexchange.[10,11] This decay constant is small (high conductivity) in comparison to tunneling through most single molecules.[11−14] On the other hand, the positive bias part is essentially independent of nanorod thickness. This clearly indicates that two different transport mechanisms are active in positive and negative bias. The exponential dependence on thickness seen in negative bias is a clear indicator of a tunneling process. This is further supported by the fact that $I-V$ curves taken from single rods at 300 and 90 K are similar, ruling out strongly thermally activated processes.

If one looks at regions off the nanorods on HOPG, one finds islands of monolayers with small clusters of molecules atop the monolayer. The area covered by a monolayer and the cleanliness of the monolayer can be greatly improved (at the cost of decreased nanorod deposition) by decreasing the concentration of porphyrin in the adsorption solution to 1 μM. A small part of one such region

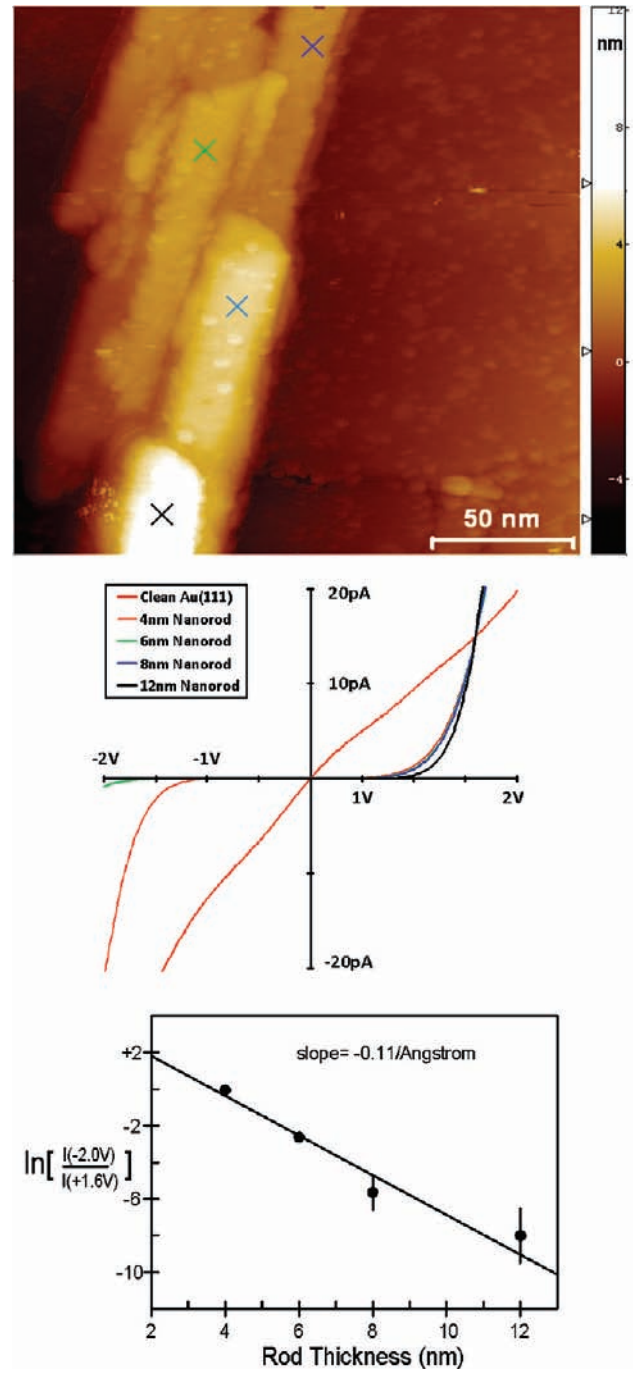

Figure 2. Constant current UHV-STM image of a nanorod on HOPG (1.6 V and 1pA). The $I-V$ curves collected at the appropriately colored points are shown in the middle (1.6 V and 15 pA). Also shown is the $I-V$ curve taken with the same tip on clean Au(111). The bottom graph is a plot showing the decrease in negative bias current.

is shown in Figure 3. At higher resolution it is possible to clearly observe the internal structure and see the saddling of the porphyrin induced by the protonation of the central nitrogen atoms. In Figure 3, it is just possible to observe the central fold in the molecular structure.

The OMTS of the monolayer and the computed dI/dV for a 12 nm thick nanorod bundle are shown in Figure 4. The peak at +1.3 V bias in Figure 4 (~3.75 eV below the vacuum level) is 0.3 eV below the observed LUMO of nickel tetraphenylporpherin, NiTPP, on Au(111).[7,15] This is consistent with the fact that the first reduction potential of H_2TSPP lies ~0.5 V deeper than that of

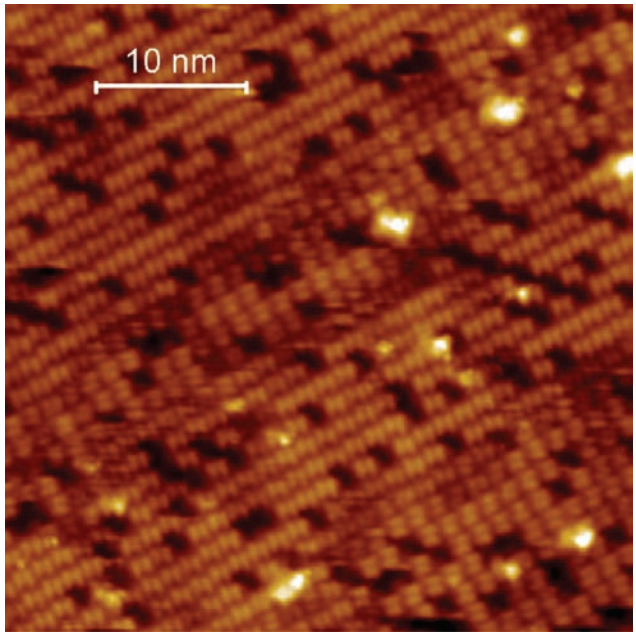

Figure 3. Constant current UHV-STM image of a monolayer of $H_2[H_4TSPP]$ on HOPG. The set point was 1 pA at +1.6 V.

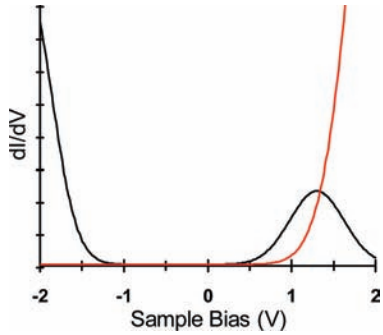

Figure 4. d*I*/d*V* for a 12 nm thick bundle of $H_2[H_4TSPP]$ nanorods on HOPG (red trace) and the OMTS of a monolayer of $H_2[H_4TSPP]$ on HOPG (black trace). The set point was 15 pA at +1.6 V.

H_2TPP and NiTPP in solution phase.[16,17] Thus, based either solely upon the OMTS[7] or upon the similarity with first reduction potentials, we assign the OMTS peak near +1.3 V bias to the LUMO of the simply adsorbed $H_2(H_4TSPP)$. Similarly, the upturn in the OMTS near −1.5 V bias (6.5 V below the vacuum level) is close to the upturn seen in NiTPP OMTS and is associated with the onset of the resonant tunneling through the HOMO.[15] Further support for these assignments is given by the fact that the Soret band of the NiTPP lies at 417 nm and that of monomeric $H_2[H_4TSPP]$ is at 434 nm, indicating that the energy difference between HOMO and LUMO is similar in both compounds.

The surface density of states can be extracted directly from the d*I*/d*V* curve only when the principal conduction mechanism is tunneling. The red trace in Figure 4 is simply the transverse conductivity of the nanorods. On the other hand, the onset of conductivity does provide insight into the energy of the associated bands. The fact that the onset of conductivity in the nanorod occurs at higher energy than the monomer may reflect a shift in energy associated with packing into the nanorod.

Based on the above monolayer assignments, it is possible to understand the rectifying behavior of the nanorods. In the case of negative bias, charge transport is entirely via a tunneling mechanism and is short range.[10,11] In positive bias the LUMO contributes to a band with relatively high conductivity such that (over 12 nm) no decrease in conductance is observed. Because the conductivity is not significantly quenched at 90 K, either the conduction mechanism is not thermally activated or the activation energy is of the order of 10 mV. This type of behavior is often associated with either metallic or resonance tunneling.[10,11] As was suggested by Schwab,[6] this is consistent with a strong overlap between LUMOs of the molecules making up the nanorods to produce a wide conduction band. However, without an accurate molecular structure for the rods, it is not possible to demonstrate why this occurs. The results presented here and by Schwab indicate that self-assembled porphyrin nanostructures have a rich treasure of optical, electronic, and optoelectronic properties that await discovery.

The data presented relate to transverse conduction in these nanorods. The effects of scattering centers, impurities, and physical defects are minimized because of the very short path length. The role that imperfections and transport direction plays in conduction is a critical one for any practical applications of this intriguing material. We are in the process of performing conductivity studies on nanorods in the longitudinal direction.

Acknowledgment. This material is based upon work supported by the National Science Foundation under Grants CHE-0555696, CHE-0848511, and DEG-0806677-004.

References

(1) Medforth, C. J.; Wang, Z.; Martin, K. E.; Song, Y.; Jacobsen, J. L.; Shelnutt, J. A. *Chem. Commun.* **2009**, *47*, 7241–7428.
(2) Friesen, B. A.; Nishida, K. R. A.; McHale, J. L.; Mazur, U. *J. Phys. Chem. C* **2009**, *113*, 1709–1718.
(3) Shimidzu, T.; Segawa, H.; Wu, F.; Nakayama, N. *J. Photochem. Photobiol., A* **1995**, *92*, 121–127.
(4) Liu, C.; Tang, H.; Bard, A. J. *J. Phys. Chem.* **1996**, *100*, 3587–3591.
(5) Fox, M. A.; Bard, A. J. *Science* **1993**, *261*, 897–899.
(6) Schwab, A. D.; Smith, D.; Bond-Watts, B.; Johnston, D.; Hone, J.; Johnson, A.; de Paula, J.; Smith, W. *Nano Lett.* **2004**, *4*, 1261–1265.
(7) Hipps, K. W.; Scudiero, L. *J. Chem. Educ.* **2005**, *82* (5), 704–711.
(8) Vlaming, S. M.; Augulls, R.; Stuart, M. C. A.; Knoester, J.; Loosdrecht, P. H. M. *J. Phys. Chem. B* **2009**, *113*, 2273–2283.
(9) Medforth, C. J.; Wang, Z.; Martin, K. E.; Song, Y.; Jacobsen, J. L.; Shelnutt, J. A. *Chem. Commun.* **2009**, *47*, 7241–7428.
(10) Segal, D.; Nitzan, A.; Davis, W. B.; Wasielewski, M. R.; Ratner, M. A. *J. Phys. Chem. B* **2000**, *104*, 3817–3829.
(11) Holmlin, R. E.; Haag, R.; Chabinyc, M. L.; Ismagilov, R.; Cohen, A.; Terfort, A.; Rampi, M.; Whitesides, G. M. *J. Am. Chem. Soc.* **2001**, *123*, 5075–5085.
(12) Sedghi, G.; Sawada, K.; Esdaile, L. J.; Hoffmann, M.; Anderson, H. L.; Bethell, D.; Haiss, W.; Higgins, S. J.; Nichols, R. J. *J. Am. Chem. Soc.* **2008**, *130*, 8582–8583.
(13) Wold, D. J.; Haag, R.; Rampi, M. A.; Frisbie, C. D. *J. Phys. Chem. B* **2002**, *106*, 2813–2816.
(14) Hirota, S.; Itoh, U.; Takada, K. *Thin Solid Films* **1988**, *165*, 337–345.
(15) Scudiero, L.; Barlow, D. E.; Mazur, U.; Hipps, K. W. *J. Am. Chem. Soc.* **2001**, *123*, 4073–4080.
(16) *The Porphyrins*; Dolphin, D., Ed.; Academic Press: New York, 1978; pp 143−144.
(17) Maiti, N. C.; Mazumdar, S.; Periasamy, N. *J. Porphyrins Phthalocyanines* **1998**, *2*, 369–379.

JA103078Q